metals

MDPI

Article

Interface Structure and Mechanical Properties of 7075Al Hybrid Composite Reinforced with Micron Ti Metal Particles Using Pressure Infiltration

Yixiong Liu [1,2,*], Zhenxing Zheng [1,*], Genghua Cao [1], Dezhi Zhu [2], Chao Yang [2] and Mingqiang Luo [3]

1 School of Mechanical and Electronic Engineering, Guangdong Polytechnic Normal University, Guangzhou 510665, China
2 Guangdong Key Laboratory for Advanced Metallic Materials processing, South China University of Technology, Guangzhou 510640, China
3 National Enterprise Technology Center, Guangdong Xingfa Aluminum (jiangxi) Co. Ltd., Yichun 336000, China
* Correspondence: liuyixiong@gpnu.edu.cn (Y.L.); zhengzhenxing@sina.com (Z.Z.); Tel.: +86-20-3882-5696 (Y.L.); +86-20-3825-7155 (Z.Z.)

Received: 30 May 2019; Accepted: 4 July 2019; Published: 8 July 2019



Abstract: Micron Ti metal particles were incorporated into SiCp/7075Al composites using pressure infiltration. The interface structure between the Ti metal particles and the matrix during the casting processes were investigated. Results show that the dispersed unreacted Ti particles form mutual diffusion layer at the interface without the formation of low-temperature intermetallic phases during the solidification processes. The interaction between the micron Ti and the molten aluminum alloy is subject to the mutual diffusion coefficient of Ti–Al rather than the reaction activation energy. The tensile strength and plasticity of the composite were improved simultaneously due to the high interfacial bonding strength and released thermal misfit stress cause by the incorporated Ti metal particles.

Keywords: aluminum matrix composite; interface; microstructure; mechanical property; hybrid

1. Introduction

The hard and brittle ceramic particles in the matrix alloy allow the aluminum matrix composites a good combination of high specific strength, high specific modulus and good wear resistance [1]. Ceramic particles, such as SiC [2], TiC [3] and Al_2O_3 [4] so on, have been widely used. However, defects, such as agglomeration, porosity and insufficient interfacial bonding, occur due to the poor wettability between the ceramics and the matrix, which severely limits their engineering application. Even though pressure infiltration could overcome the adverse capillary forces due to poor wettability utilizing applied load and is usually employed to produce composites of high microstructural quality, rapidly [5]. Extra ceramic surfaces modification is still adopted to improve wettability at aluminum/ceramic interfaces and reduce the threshold pressure for infiltration. A. Alonso et al. found that the addition of only a 2 wt% of K_2ZrF_6 compound promoted a 45% decrease in the threshold pressure [6]. The interfaces between the ceramics and aluminum have great influences on the mechanical performance of the composites. M. Kouzeli and C. S. Marchi found that the contiguity of the reinforcement, due to the reaction between the B_4C and aluminum matrix, not only increased the composite flow stress, but also resulted in a higher rate of particle fracture, significantly influenced the mechanical behaviors of the composite [7].

Another way to overcome these adverse effects is to use metal reinforcements [8–10]. Metal reinforcements, such as metallic glasses [11,12], quasi-crystalline [13], alloy [14,15], intermetallics [16] and pure metal [17] so on, are considered by researchers to negate the adverse effects associating with ceramics. Available scientific literatures have been revealed that plasticity metallic reinforcements could improve the strength and plasticity of composites [18–21]. Liu et al. found that transition layer formed during the sintering of AlCoCrFeNi high-entropy alloy/Al composites [15]. The transition layer is favorable for the transformation of the stress state from the iso-stress condition to the iso-strain condition for the composites during the deformation process, which improved both yield strength and ductility of the composites. High interfacial bonding strength can be easily obtained for the metal reinforcements due to their better wettability with the aluminum matrix alloy [22]. Gao et al. prepared A356 composites reinforced with Ti particles utilizing powder thixoforming method [10]. The formed Ti@(Al-Si-Ti) core- shell-structured particles in the composite decreased crack size in the shell, delayed crack propagation by plastic deformation and multiplied secondary cracks, leading to excellent ductility of the composites. While in the research made by Chen et al., Ti particles entirely reacted with the 2024Al melts during the casting processes. The compression and tensile strengths were both increased gradually at the sacrifice of plasticity due to the mass fraction of Al_3Ti existence [23]. There is no doubt that the interface of the metal reinforcements plays a vital role in determining the microstructure and mechanical properties of the composites. So far, most aluminum matrix composites reinforced with metal particles usually use low temperature fabrication techniques to restrict the possible reactions between the metal reinforcements and the matrix. Seldom researches have been made to investigate the interfacial interaction between micron metal particles and molten alloy until now.

In the current study, pressure infiltration was employed to prepare high quality aluminum matrix composites with micron Ti metal particles incorporated. Interface between the metal Ti particles and molten aluminum alloy was characterized and investigated. The effects of Ti metal particles on the mechanical behaviors of the composites were discussed.

2. Methods and Experiments

Figure 1 shows the morphologies of the reinforcements used here. SiC particles (purity ≥99.1%, Shanghai chaowei nano technology co., LTD) in two different sizes and a Ti particle (purity ≥99.1%, Beijing Goodwill Metal Tech Co. LTD, Beijing, China) were used. The SiC particle is in an average size of 7 μm (D(10) = 4.2 μm, D(50) = 7 μm and D(90) = 11.4 μm) and 35 μm (D(10) = 22.1 μm, D(50) = 35 μm and D(90) = 55.7 μm), respectively. The average size of Ti metal particles is 35 μm (D(10) = 10.8 μm, D(50) = 35 μm and D(90) = 78.8 μm), in the same size with the larger SiC particles. Commercial 7075Al was used as the matrix alloy. Table 1 lists the chemical compositions of 7075Al.

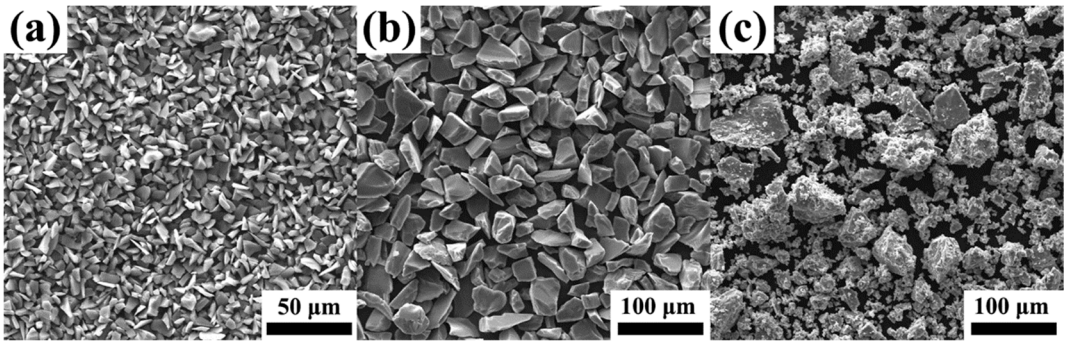


Figure 1. The morphologies of the reinforcements used here: (**a**) 7 μm SiC particles; (**b**) 35 μm SiC particles and (**c**) 35 μm Ti metal particles.

Table 1. Chemical compositions (weight percent) of 7075Al.

Alloy	Si	Fe	Cu	Mn	Mg	Cr	Zn	Ti	Others	Al
7075Al	0.046	0.109	1.333	0.027	2.085	0.225	5.614	0.009	0.038	Balanced

7075Al hybrid composites were fabricated using pressure infiltration method. Figure 2 displays the fabricating processes. At first, 7 μm SiC particles and 35 μm Ti metal particles were weighted and put into a corundum vial together with corundum balls. The corundum vial was sealed and rotated in a tumbling mill for 10 h at a rotation speed of 110 rpm. The Ti particles and SiC particles is in a volume ratio of 1:8. Then the mixture was prepacked into Φ 80 × 40 mm^2 and settled into a mold. 7075Al melts at 780 °C was poured into the mold and pressure infiltrated into the preform at 580 °C using a piston. The pressure is about 50 MPa and holding for 5 min after the infiltration processes completed. Subsequently, the as-casting together with the mold were water cooled down to room temperature in 30 min. Finally, 7075Al hybrid composites reinforced with 40 vol.% 7 μm SiCp and 5 vol.% 35 μm Ti particles, hereafter referred to as AMC-Ti, were fabricated. The fabricated composite billets were in a size of Φ 80 × 40 mm^2. For comparison, 7075Al composites reinforced with 40 vol.% 7 μm SiCp and 5 vol.% 35 μm SiCp, hereafter referred to as AMC-SiC, were also fabricated under the same conditions.

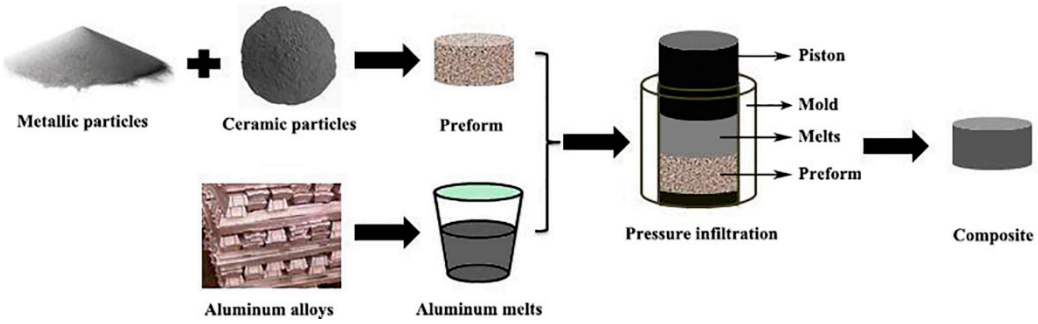


Figure 2. Fabricating processes of composites.

Flat dog-bone tensile test specimens, with a rectangular cross section of 5 × 2 mm^2 and a gauge length of 15 mm (Figure 3), were tested at room temperature using an INSTRON 5569 testing system (INSTRON, Boston, MA, USA) with a cross-head speed of 0.5 mm/min. The strain was recorded by an extensometer attachment with a gauge length of 10 mm. The test results were taken an average of five specimens for mechanical property analysis.

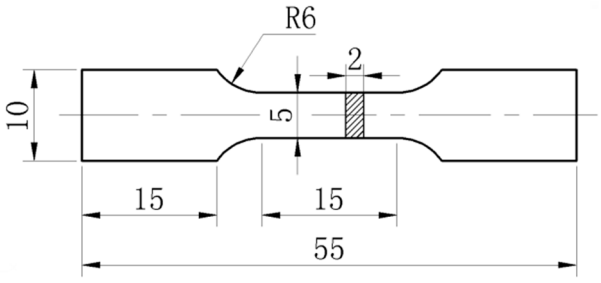


Figure 3. Dimension of the specimen for tensile testing (unit: mm).

The morphologies of the composites were characterized using a Quanta 200 scanning electron microscopy (SEM; FEI, Eindhoven, The Netherlands) and a Tecnai G2 F20 field emission gun transmission electron microscopy (TEM; FEI, Portland, OR, USA) coupled with an energy-dispersive X-ray analysis. X-ray diffraction (D8 Advance; Bruker, Karlsruhe, Germany) was used to identify the possible formed phases during the solidification of the composites.

3. Results and Discussion

Figure 4 depicts the SEM pictures of the composites. As shown in Figure 4, no obvious porous and particle agglomeration are detected. Reinforcements are homogeneously distributed in 7075Al matrix. The interfaces between the Ti metal particles and 7075Al matrix are clear (Figure 4b). Interfacial reaction product is inconspicuous in the vicinity of Ti metal particles. The observed results indicate a limited interfacial reaction between the Ti metal particles and the 7075Al melts during the fabricating processes.

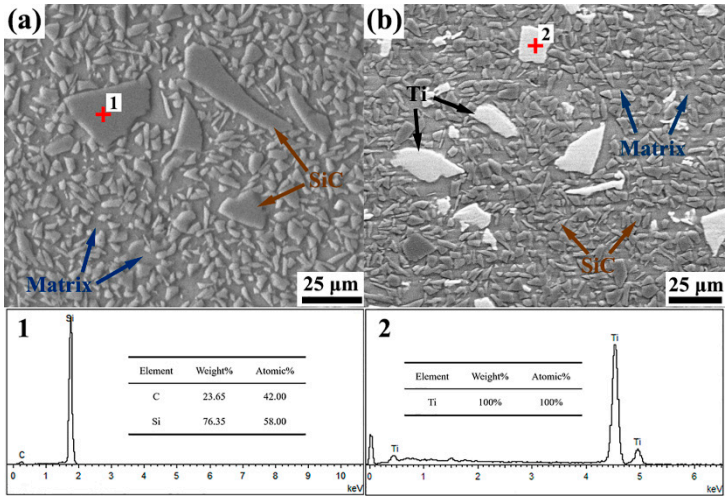


Figure 4. SEM microstructure of the prepared composites: (**a**) AMC-SiC composite; (**b**) AMC-Ti composite.

Figure 5 shows the energy spectrum analysis of the Ti–Al interface. A transition layer can be detected in the vicinity of the Ti metal particles (Figure 5b). The transition layer comprises two regions (Figure 5c). Mutual diffusion between the Ti metal particle and the matrix happened during the preparing processes (Figure 5c, region I). In addition, Mg atoms are detected in the edge of the Ti metal particles. Mg atoms segregate at the interface of the Ti metal particle and diffuse into Ti metal particle (Figure 5c, region I and II). It is remarked that mutual diffusion between the Ti metal particle and the molten 7075Al occur without a specific atom ratio.

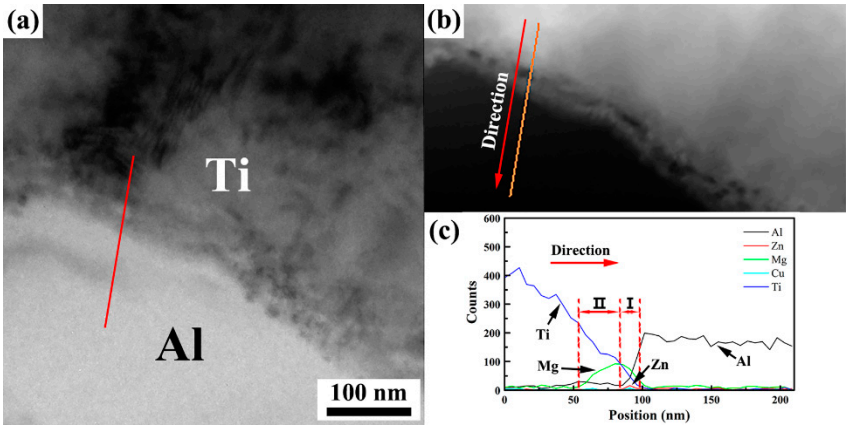


Figure 5. Energy spectrum analysis of the Ti–Al interface: (**a**) Bright-field TEM image of Ti–Al interface; (**b**) HAADF STEM image of Ti–Al interface and (**c**) line scan analysis of Ti–Al interface.

To clarify the interfacial structure between the Ti metal particles and the matrix, high resolution transmission electron microscopy was used. Three continuous areas of the interface were selected. Fourier transform (FFT) and inverse Fourier transform were used to analyze the interface structure. Compared with the diffraction spectrums of the selected area closing to the Ti metal particle,

the diffraction spectrums of the selected area analyzed by FFT in the vicinity of the matrix is irregularity (Figure 6a,c,e), indicating a neither amorphous nor crystal structure. Long-range order structure of Ti_xAl_y low temperature phases could not be detected in the interface as shown in the inverse FFT results (Figure 6b,d,f). Numerous defects, such as lattice distortion, point defect, line defect, etc., can be easily detected in the corresponding inverse FFT results as the arrows and ellipses shown in Figure 6b,d,f. These defects are generated as a result of the mutual diffusion of the Ti, Mg and Al atoms. The generated defects in the mutual diffusion layer ultimately ensure a high interfacial bonding strength between the Ti metal particle and the matrix, which would exert positive effects on the load transfer effects of the interface in vicinity of Ti metal particles in the end. Finally, metallurgical bonding between the Ti metal particle and the matrix was formed during the casting solidification process.

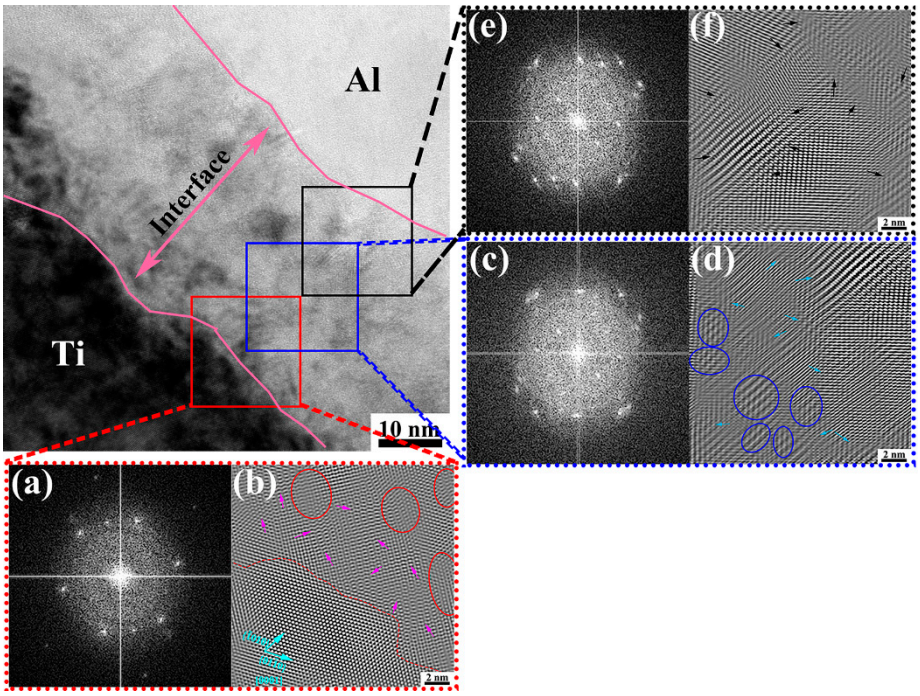


Figure 6. Analysis of the Ti–Al interface: (**a**,**c**,**e**) Fourier transformed pattern of the selected areas; and (**b**,**d**,**f**) the corresponding inverse Fourier transformed pattern of the selected areas.

Figure 7 shows the X-ray diffraction patterns of the prepared composites. The X-ray diffraction pattern results of the composites are fully consistent with the aforementioned experimental results. Apart from the diffraction peak of the main constitutes of AMC-Ti composites, the diffraction peak of the possible formed low temperature intermetallic compound is not detected in the figure. Once again, it is confirmed that Ti metal particles did not react with aluminum alloy melts to form low-temperature intermetallic compound phases in the process of pressure infiltration.

As it well known, a reaction is controlled by the activation energy and reaction rate. Despite the activation energy of the phases formation, the reaction between the incorporated Ti metal particles and aluminum melts is also controlled by mutual diffusion coefficient and reaction time. The impurity diffusion coefficient is usually described by the Arrhenius equation:

$$D = D_0 \cdot \exp(-Q/RT), \quad (1)$$

where D_0 is denoted as the pre-exponential factor and Q as the activation energy. T denotes the absolute temperature and R the gas constant. Thus the values of the diffusion coefficients for the liquid Al in the solid Ti ($D_{Al/Ti}$), the solid Ti in the liquid Al ($D_{Ti/Al}$) can be calculated and are about 3.3×10^{-19} m^2/s and 6.8×10^{-9} m^2/s, respectively according to the parameters in Table 2. This result illustrates that

solid Ti is the main diffusing species in the Al(l)–Ti(s) system, for the value of $D_{Ti/Al}$ is larger than that of $D_{Al/Ti}$ by round ten orders of magnitude. Moreover, the solubility of Ti atom in the Al melt is rather low in the temperature range of 760–800 °C as the Ti–Al binary phase diagram shown in Figure 8. The analysis corroborates that the mutual diffusion between the Ti metal particle and the molten 7075Al melts is inconspicuous due to their low mutual diffusion coefficient and limited reaction time. Finally, the interaction between the Ti metal particle and the molten 7075Al melts is restricted and the thickness of interface layer is thin in the end.

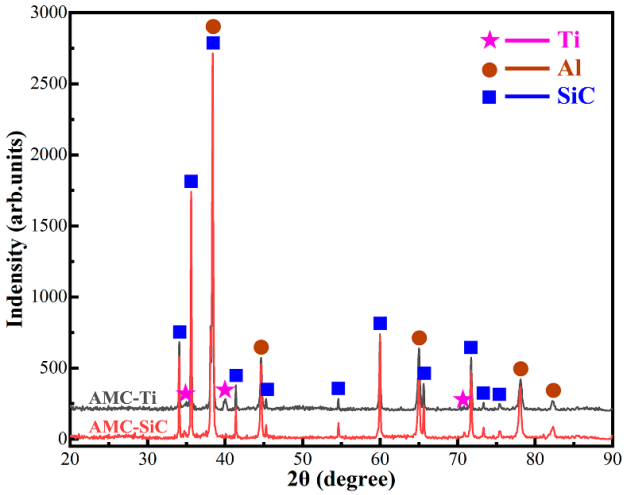


Figure 7. XRD patterns of the prepared composites.

Table 2. Assessed Arrhenius parameters for impurity diffusion coefficients in liquid Al.

Solute	Solvent	D_0 (m^2/s)	Q (KJ/mole)	Temperature Range (K)	Reference
Ti	Al	4.29×10^{-7}	36.3	850–1100	[24]
Al	Ti	6.6×10^{-3}	329 ± 2	850–1100	[25]

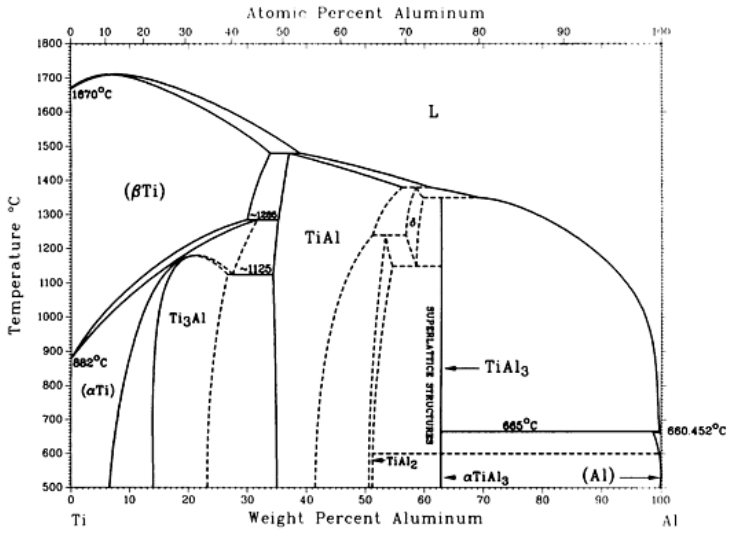


Figure 8. Phase diagram Ti–Al [26].

Figure 9 displays the stress–strain curves of the prepared composites. It can be seen that the AMC-Ti composites achieve higher average tensile strength and plasticity than the AMC-SiC composites (Table 3). The AMC-Ti hybrid composites have a strength of 605 MPa, which is 148 MPa higher than that of the AMC-SiC hybrid composites (Figure 9). Besides, the plasticity of the AMC-Ti hybrid

composites reaches 1.28%, improving 235% when it is compared with that of the AMC-SiC composites (Figure 9). Obviously, the incorporated Ti metal particles improve the strength and plasticity of the composites simultaneously.

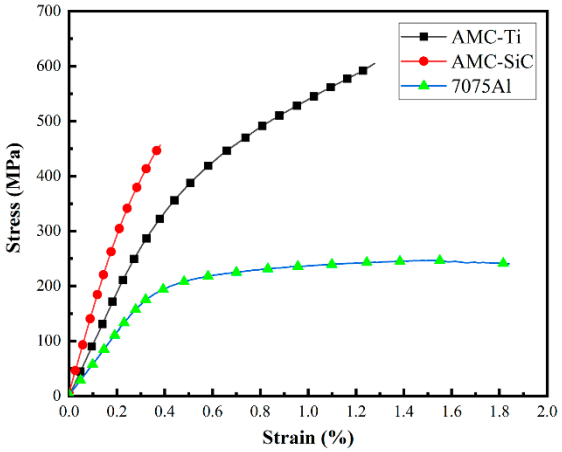


Figure 9. Engineering stress–strain curves of the prepared composites and the matrix.

Table 3. Tensile properties of the prepared composites in as-casting.

Materials	E (GPa)	σ_y (MPa)	σ_{max} (MPa)	ε_f (%)
AMC-SiC	155 ± 10	423 ± 27	460 ± 19	0.39 ± 0.05
AMC-Ti	100 ± 13	488 ± 33	623 ± 17	1.20 ± 0.13

The fracture morphologies of the composites are observed to study the fracture behaviors of the composites (Figure 10). Apparent differences in fracture morphology between AMC-SiC hybrid composites and AMC-Ti hybrid composites can be detected. The fracture morphology of AMC-SiC hybrid composites is plain and simple and transgranular fractures of larger SiC particles are easily detected on the fracture surface (Figure 10a,b). Moreover, torn edges formed in the matrix alloy of AMC-SiC hybrid composites during the tensile tests is shallow and blunt (Figure 10c). On the contrary, the fracture morphologies of the AMC-Ti hybrid composites are dramatically different from those of the AMC-SiC hybrid composites, which indicate a mixed feature of ductile–brittle fracture, not a typical brittle fracture or a typical ductile fracture. The fracture surface is fluctuating and much more complex than that of the AMC-SiC hybrid composites (Figure 10a,d). Fractured Ti metal particles can be easily detected at the fracture surface of AMC-Ti composites. It can be deduced that the high interfacial bonding strength of the Ti–Al interface ensures the load effectively transfer to the Ti metal particles during the deformation, leading to an improvement of tensile strength of the AMC-Ti composites. Moreover, small ductile dimples and abundant torn edges are clearly visible in the matrix alloy of AMC-Ti hybrid composites as shown in Figure 10f. The observed ductile dimples and torn edges are consistent with the plasticity results discussed above.

It is widely accepted that thermal misfit stress would generate around the incorporated reinforcements with a change in temperature for the dissimilar coefficients of thermal expansion between the reinforcements and the matrix [27]. With a view to the interaction between the reinforcement and the matrix, dislocations would come about in the vicinity of the SiC particles due to the generated thermal misfit compressive stress (Figure 11a). On the contrary, dislocations are hardly detected in the vicinity of the Ti particles (Figure 11b). A detailed discussion of the interaction between the generated dislocations and the reinforcements can be found in Ref. [28]; here we shall only comment on points relevant to the interactions between the reinforcements.

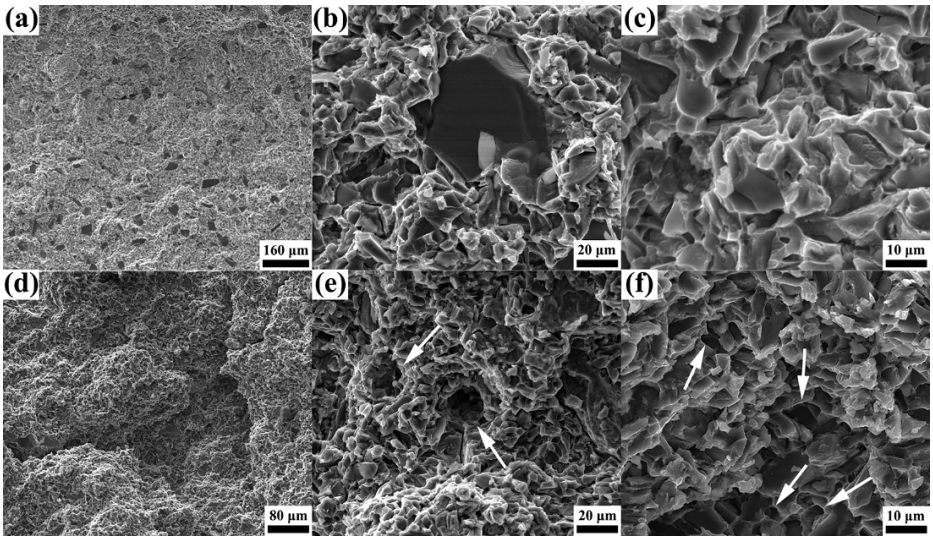


Figure 10. Representative tensile fracture morphologies of the composites: (**a**–**c**) Fracture surfaces of AMC-SiC hybrid composites; and (**d**–**f**) fracture surfaces of AMC-Ti hybrid composites.

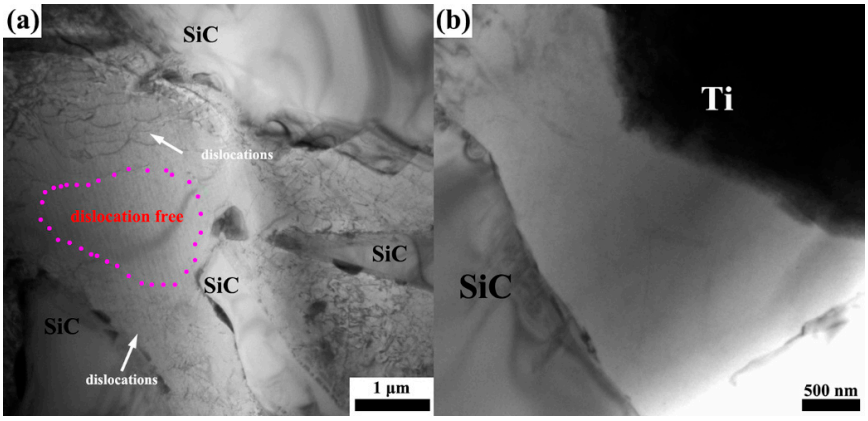


Figure 11. TEM of the composites: (**a**) AMC-SiC composites; and (**b**) AMC-Ti composites.

Undoubtedly, the matrix acts as the medium for interactions between the reinforcements. Considering the interactions with other particles, balanced high tensile stresses occur in the matrix ligament closely sandwiched between two SiC particles [27] (Figure 12). As a result, dislocation reduced greatly in the matrix ligament closely sandwiched between two SiC particles (Figure 11a). While in the case of the Ti metal particles, the dislocations disappeared from the interface of the SiC particles nearby the Ti particles as well (Figure 11b). The balanced tensile stresses in the matrix ligament closely sandwiched between the Ti metal particle and SiC particle are lower than that between two SiC particles (Figure 12). The lower balanced tensile stresses between Ti metal particles and the matrix would impede the formation and propagation of the cracks in the matrix and can be beneficial to the mechanical strength of the composites (Figure 9). Besides, the plastic deformation of the matrix in the composites containing Ti metal particles would be also greater than that of the composites without Ti metal particles addition (Figure 10). As a result, small ductile dimples and abundant torn edges are clearly visible in the matrix alloy of AMC-Ti hybrid composites (Figure 10). Moreover, the mutual diffusion Ti–Al interfaces ensure the collaborative deformation of the Ti metal particles and the matrix before the Ti metal particles cracked. Finally, the plasticity of AMC-Ti composites is improved (Figure 9). Obviously, the fracture behaviors of the composites have been greatly influenced by the incorporated Ti metal particles and the interface between the Ti metal particles and the matrix. The incorporated Ti metal particles would exert positive effects on the mechanical performance of the composites.

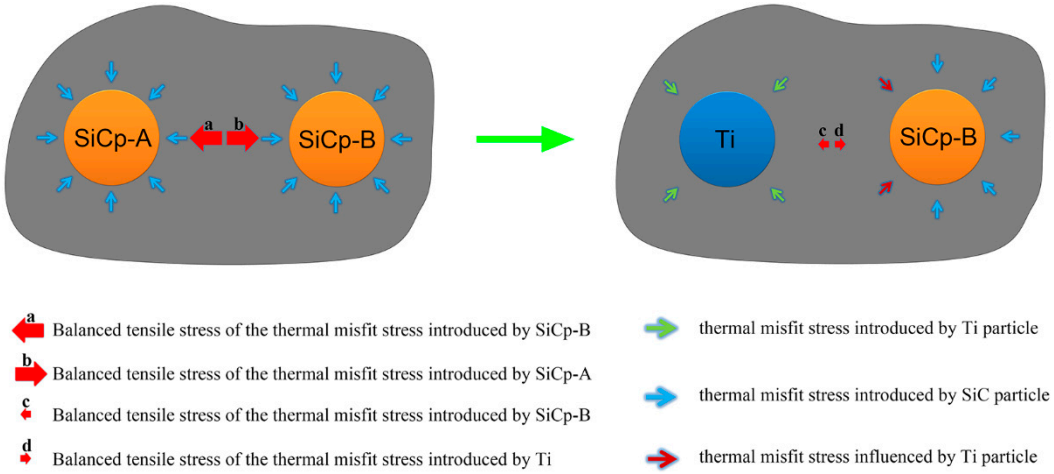


Figure 12. Schematic diagram of the influence of Ti particle on the thermal misfit stress in matrix.

4. Conclusions

In this work, the interface structure and mechanical properties of 7075Al hybrid composite reinforced with micron Ti metal particles using pressure infiltration were investigated. The incorporated Ti particles in the hybrid composites improved the tensile strength and plasticity of the composites. The fracture behaviors of the composites were influenced. From the experimental results, the following conclusions can be concluded:

1. Ti metal particles remained during the pressure infiltration processes. No additional low temperature phases were generated at the interface of the Ti metal particles. Numerous defects generated due to the mutual diffusion of the Ti metal particles and the molten 7075Al melts. The formed metallurgical bonding between the Ti metal particles and the matrix ensures high interfacial bonding strength between the Ti metal particle and the matrix.
2. The reaction between the incorporated Ti metal particles and aluminum melts was controlled by the mutual diffusion coefficient and reaction time rather than the activation energy of the low temperature phases. Solid Ti is the main diffusing species in the Al(l)–Ti(s) system. The interaction between the Ti metal particle and the molten 7075Al melts was restricted due to the low solubility of the Ti atom in the Al melt.
3. The matrix acts as the medium for interactions between the incorporated reinforcements. The balanced tensile stresses in the matrix ligament closely sandwiched between the Ti metal particle and SiC particle was lower than that between two SiC particles, which impedes the formation and propagation of the cracks in the matrix and result in an improvement in plastic deformation of the matrix. Moreover, the mutual diffusion Ti–Al interfaces ensure the load transfer effects and the collaborative deformation of the Ti metal particles and the matrix. The incorporated Ti metal particles can be beneficial to the mechanical performance of the composites.

Author Contributions: Conceptualization, Y.L. and Z.Z.; methodology, D.Z.; investigation, Y.L. and Z.Z.; resources, D.Z. and C.Y.; data curation, G.C. and M.L.; writing—original draft preparation, Y.L. and Z.Z.; writing—review and editing, Y.L. and G.C.; project administration, Y.L. and C.Y.; funding acquisition, Y.L.

Funding: This research was funded by Guangdong Provincial Young Innovation Talents Project, grant number 2016KQNCX094, Guangdong Matural Science Fund Project, grant number 2015A030313668, Guangdong Science and Technology Planning Project, grant number 2017B090913006, and Guangdong Engneering Technology Research Center, grant number 2017GCZX003.

Conflicts of Interest: The authors declare no conflict of interest.

References

1. Lee, H.; Choi, J.H.; Jo, M.C.; Lee, D.; Shin, S.; Jo, I.; Lee, S.-K.; Lee, S. Effects of SiC particulate size on dynamic compressive properties in 7075-T6 Al-SiC_p composites. *Mater. Sci. Eng. A.* **2018**, *738*, 412–419. [CrossRef]
2. Xu, Q.; Ma, A.; Wang, J.; Sun, J.; Jiang, J.; Li, Y.; Ni, C. Development of high-performance SiC_p/Al-Si composites by equal channel angular pressing. *Metals* **2018**, *8*, 738. [CrossRef]
3. Hadian, M.; Shahrajabian, H.; Rafiei, M. Mechanical properties and microstructure of Al/(TiC+TiB_2) composite fabricated by spark plasma sintering. *Ceram. Int.* **2019**, *45*, 12088–12092. [CrossRef]
4. Zan, Y.N.; Zhou, Y.T.; Liu, Z.Y.; Ma, G.N.; Wang, D.; Wang, Q.Z.; Wang, W.G.; Xiao, B.L.; Ma, Z.Y. Enhancing strength and ductility synergy through heterogeneous structure design in nanoscale Al_2O_3 particulate reinforced Al composites. *Mater. Des.* **2019**, *166*, 107629. [CrossRef]
5. Léger, A.; Weber, L.; Mortensen, A. Influence of the wetting angle on capillary forces in pressure infiltration. *Acta Mater.* **2015**, *91*, 57–69. [CrossRef]
6. Alonso, A.; Narciso, J.; Pamies, A.; Garcia-Cordovilla, C.; Louis, E. Effect of K_2ZrF_6 coatings on pressure infiltration of packed SiC particulates by liquid aluminum. *Scr. Metall. Mater.* **1993**, *29*, 1559–1564. [CrossRef]
7. Kouzeli, M.; San Marchi, C.; Mortensen, A. Effect of reaction on the tensile behavior of infiltrated boron carbide-aluminum composites. *Mater. Sci. Eng. A.* **2002**, *337*, 264–273. [CrossRef]
8. Ali, F.; Scudino, S.; Liu, G.; Srivastava, V.C.; Mukhopadhyay, N.K.; Khoshkhoo, M.S.; Prashanth, K.G.; Uhlenwinkel, V.; Calin, M.; Eckert, J. Modeling the strengthening effect of Al-Cu-Fe quasicrystalline particles in Al-based metal matrix composites. *J. Alloys Compd.* **2012**, *536*, S130–S133. [CrossRef]
9. Jang, J.S.C.; Li, T.H.; Jian, S.R.; Huang, J.C.; Nieh, T.G. Effects of characteristics of Mo dispersions on the plasticity of Mg-based bulk metallic glass composites. *Intermetallics* **2011**, *19*, 738–743. [CrossRef]
10. Gao, M.; Chen, T.; Qin, H. Effects of mold temperature on the microstructure and tensile properties of Ti@(Al-Si-Ti)p/A356 composite prepared via powder thixoforming. *Metals* **2018**, *8*, 829. [CrossRef]
11. Zhang, W.; Hu, Y.; Zhang, G.; Wang, Z. Formation of nanoscale metallic glassy particle reinforced Al-based composite powders by high-energy milling. *Metals* **2017**, *7*, 425. [CrossRef]
12. Rezaei, M.R.; Shabestari, S.G.; Razavi, S.H. Effect of ECAP consolidation temperature on the microstructure and mechanical properties of Al-Cu-Ti metallic glass reinforced aluminum matrix composite. *J. Mater. Sci. Technol.* **2017**, *33*, 1031–1038. [CrossRef]
13. Kang, N.; Fu, Y.; Coddet, P.; Guelorget, B.; Liao, H.; Coddet, C. On the microstructure, hardness and wear behavior of Al-Fe-Cr quasicrystal reinforced Al matrix composite prepared by selective laser melting. *Mater. Des.* **2017**, *132*, 105–111. [CrossRef]
14. Zhou, C.; Zhang, Q.; Tan, X.; Deng, S.; Shi, K.; Wang, C.; Wu, G. Fully-dense Mn3Zn0.7Ge0.3N/Al composites with zero thermal expansion behavior around room temperature. *Materialia* **2019**, *6*, 100289. [CrossRef]
15. Liu, Y.; Chen, J.; Li, Z.; Wang, X.; Fan, X.; Liu, J. Formation of transition layer and its effect on mechanical properties of AlCoCrFeNi high-entropy alloy/Al composites. *J. Alloys Compd.* **2019**, *780*, 558–564. [CrossRef]
16. Rasouli, M.; Akhlaghi, F.; Ojo, O.O.; Paidar, M. Preparation and characterization of in-situ Al-Al_XNi_Y composites via reactive infiltration. *J. Alloys Compd.* **2019**, *780*, 829–845. [CrossRef]
17. Rezaei, A.; Madaah Hosseini, H.R. Evolution of microstructure and mechanical properties of Al-5wt% Ti composite fabricated by P/M and hot extrusion: Effect of heat treatment. *Mater. Sci. Eng. A.* **2017**, *689*, 166–175. [CrossRef]
18. Yadav, D.; Bauri, R. Nickel particle embedded aluminium matrix composite with high ductility. *Mater. Lett.* **2010**, *64*, 664–667. [CrossRef]
19. Pandey, A.B.; Majumdar, B.S.; Miracle, D.B. Effect of aluminum particles on the fracture toughness of a 7093/SiC/15p composite. *Mater. Sci. Eng. A.* **1999**, *259*, 296–307. [CrossRef]
20. Markó, D.; Prashanth, K.G.; Scudino, S.; Wang, Z.; Ellendt, N.; Uhlenwinkel, V.; Eckert, J. Al-based metal matrix composites reinforced with Fe49.9Co35.1Nb7.7B4.5Si2.8 glassy powder: Mechanical behavior under tensile loading. *J. Alloys Compd.* **2014**, *615*, S382–S385. [CrossRef]
21. Lu, T.; Chen, W.; Xu, W.; Wang, P.; Mao, M.; Liu, Y.; Fu, Z. The effects of Cr particles addition on the aging behavior and mechanical properties of SiC_p/7075Al composites. *Mater. Charact.* **2018**, *136*, 264–271. [CrossRef]

22. Zhang, L.; Li, B.; Wu, H.; Wang, W.; Zhai, S.; Xu, J.; Niu, Z.; Wang, Y. Microstructure and property characterization of Al-based composites reinforced with CuZrAl particles fabricated by mechanical alloying and spark plasma sintering. *Adv. Powder Technol.* **2018**, *29*, 1695–1702. [CrossRef]
23. Chen, G.; Jin, Y.; Zhang, H.; Han, F.; Chen, Q.; Xu, J.; Zhao, Z. Microstructures and mechanical properties of in-situ Al_3Ti/2024Al composites after solution and subsequent aging treatment. *Mater. Sci. Eng. A.* **2018**, *724*, 181–188. [CrossRef]
24. Du, Y.; Chang, Y.A.; Huang, B.; Gong, W.; Jin, Z.; Xu, H.; Yuan, Z.; Liu, Y.; He, Y.; Xie, F.Y. Diffusion coefficients of some solutes in fcc and liquid Al: Critical evaluation and correlation. *Mater. Sci. Eng. A.* **2003**, *363*, 140–151. [CrossRef]
25. Köppers, M.; Herzig, C.; Friesel, M.; Mishin, Y. Intrinsic self-diffusion and substitutional Al diffusion in α-Ti. *Acta Mater.* **1997**, *45*, 4181–4191. [CrossRef]
26. ASM International. *ASM Handbook—Alloy Phase Diagrams*; The Materials Information Company: New York, NY, USA, 1995; p. 327.
27. Kelly, A.; Zweben, C.H. *Comprehensive Composite Materials*; Pergamon Press: New York, NY, USA, 2000; p. 35.
28. Liu, Y.; Yang, C.; Chen, W.; Zhu, D.; Li, Y. Effects of particle size and properties on the microstructures, mechanical properties, and fracture mechanisms of 7075Al hybrid composites prepared by squeeze casting. *J. Mater. Sci.* **2014**, *49*, 7855–7863. [CrossRef]



© 2019 by the authors. Licensee MDPI, Basel, Switzerland. This article is an open access article distributed under the terms and conditions of the Creative Commons Attribution (CC BY) license (http://creativecommons.org/licenses/by/4.0/).